[Article ID] 1003－6326(2002)06－1099－04

Finite element method simulation for tensile process of sintered iron-base material①

ZHAO Wei-bin(赵伟斌), LI Yuan-yuan(李元元), ZHOU Zhao-yao(周照耀),
SHAO Ming(邵 明), CHEN Wei-ping(陈维平), ZHANG Wen(张 文)
(College of Mechanical Engineering, South China University of Technology, Guangzhou 510640, China)

[Abstract] Different material properties leads to different metal fracture behaviors. Even if the powder material is composed of plastic metal, the fracture still does not show macroscopic plastic deformation characteristics if the material contains a large number of voids. Eight-node isoparametric elastic-plastic finite element method was used to simulate the tensile process of sintered powder material. By setting a number of voids in the analyzed metal cuboid, the initial density was taken into consideration. The material properties of the three-dimensional solid for the tensile simulation were defined with reference to the known pure iron material parameters. The load-displacement curves during elongation were obtained with a universal testing machine, and then the simulated curves were compared with the experimental results. The factors that cause the stress concentration and strength decrease were analyzed according to the simulated equivalent von Mises stress distribution.

[Key words] Finite element method simulation; tension; sintered powder material
[CLC number] TG 376 [Document code] A

1 INTRODUCTION

Die compaction of powder has been used in components manufacturing in different fields[1~5]. With the development of powder metallurgy, more attention is focused on improving the total performance of powder metallurgy parts. Parameters including the mechanical and material properties are usually obtained by means of experimental method. With the obtained parameters, computer simulation provides a powerful tool to analyze the deforming process of metal material.

For the analysis of the deforming process of sintered metal material, various models have been proposed to reflect the constitutive relationship[6~15]. The typical Shima's model is based on a modified von Mises yielding criterion[9]. Another approach in obtaining a suitable model for powders is to modify the existing material models used for simulating the behavior of soil. Difference between the powder and the compact metal has not been taken into consideration in the present models.

Different from the compaction process, the tensile process is no longer affected by the wall friction[5]. On the other hand, the random distribution of voids and the initial relative density were taken into account according to the designed assumption.

Since the tensile process normally involves large displacements(or tool movements), the applied force or prescribed displacements must be divided into smaller increments and the equilibrium equation has to be satisfied at each increment. Using small deformation theory, unrealistic solutions for density and stress field are usually obtained. For a realistic solution, the load increment has to be very small. Large deforming theory such as the Lagrangian[16] description of motion is more appropriate for powder deformation simulation. MSC. Marc was applied in this paper to analyze the sintered powder material[16]. Once the relevant parameters of the material were obtained, we can acquire many information including deforming and destruction, thereby reasonably explain many phenomena which occur during the deforming process, thus avoiding the waste of time and material due to repetitive experiments.

2 EXPERIMENTAL

The comparison was performed using standard sintered samples(ISO 2740－1973). Fig. 1 shows the overall dimension of the sintered sample prepared according to the national standard. Initially, the thickness C is 6.0 mm, L_c is 32 mm. After elongation, C is 5.7 mm and L_c is 37 mm. The initial relative density of the tensile sample is approximately 89.7 %.

The tensile samples were prepared from highly compressible water atomized iron powder with particle size of

① [Foundation item] Key project(50135020) supported by the National Natural Science Foundation of China; project(2001AA337010) by the National Advanced Technology Research and Development project; project([2001]No. 1) by the Ministry of Education(Excellent person for 21st Century Training Project); project(984048) by the Natural Science Foundation of Guangdong Province
[Received date] 2002－07－30; [Accepted date] 2002－11－08

100~ 150 μm. The mass of the specimen was kept constant at about 27 g. At least three other specimens were pressed afterwards under the same condition. Results show good reproducibility. The compacts were sintered at 1 120 ℃ for 2 h[1, 2, 6].

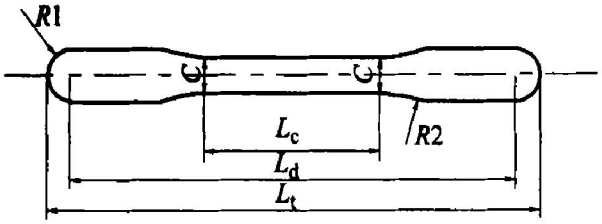

Fig. 1 Dimension of tensile sample

One edge of the sample was clamped, which prevented rigid body motion of the sample. Another clamp (upper clamp) moved at a speed of 2 mm per minute. The upper clamp was stopped when the sample was finally snapped. This occurred when the total displacement of the upper punch was 5 mm. During the deformation, the curve of the load versus the displacement was recorded by a microcomputer. The length of the sample increased, and the width reduced accordingly. The final overall dimensions were measured.

3 FEM SIMULATION

3.1 Fundamental equations

Eight-node isoparametric element method was used in this model to improve the precision of calculation.

In order to analyze the three-dimensional problem, natural coordinate system should include three dimensionless parameters ξ, η and ζ to denote the position of elemental nodes in detail.

$$-1 \leqslant \xi \leqslant 1,\ -1 \leqslant \eta \leqslant 1,\ -1 \leqslant \zeta \leqslant 1$$

The coordinate and displacement interpolation formula of eight-node isoparameteric method are as follows:

$$\begin{aligned} [u] &= [N][u^e] \\ [v] &= [N][v^e] \\ [w] &= [N][w^e] \end{aligned} \tag{1}$$

where

$$[N] = \begin{vmatrix} N_1 & 0 & N_2 & 0 & \cdots & N_m & 0 \\ 0 & N_1 & 0 & N_2 & \cdots & 0 & N_m \end{vmatrix} \tag{2}$$

The relationship between strain increment and displacement increment of elemental node is defined as follows:

$$\{d\varepsilon\} = [B]\{d\delta\} \tag{3}$$

where $[B]$ is the matrix correlating the strain.

Using the virtual work principle, the system equation becomes:

$$\begin{aligned} \phi(\delta) &= \sum \int [B]^t d\sigma dV - \Delta R = 0 \\ \{d\sigma\} &= [D_{ep}]\{d\varepsilon\} \end{aligned} \tag{4}$$

$$[D_{dp}] = [D_e] - [D_p]$$

where R is the applied force, $[D_e]$ is the usual elastic matrix with elastic modulus E and Poisson's ratio v. $[D_p]$ is the plastic matrix where the plastic characteristics of the powder are incorporated.

The universal element stiffness matrix is:

$$[K^e] = \int_{V_e} [B]^T [D_{ep}][B]\, dV \tag{5}$$

So the corresponding isoparametric element stiffness matrix in this model becomes:

$$[K^e] = \int_{-1}^{1} \int_{-1}^{1} \int_{-1}^{1} [B]^T [D_{ep}][B] |J| \, d\xi d\eta d\zeta \tag{6}$$

where $|J|$ is the Jacobi determinant of coordination transformation.

3.2 Pore distribution

The sintered powder metallurgy part was treated as a piece of normal metal with holes in it. The analyzed cuboid was assumed to be 32.0 mm long, 6.0 mm wide and 5.0 mm high. The model was built on MSC Mentat[12]. The element type selected for this analysis was Marc element type 7, an eight-noded hexahedral element. Totally there remained 5 272 elements after 928 elements were subtracted from the three-dimensional solid, so the average relative density was 87.9%, approximating to the initial relative density of the tensile sample. The assumption of the element subtraction is illustrated with Fig. 2 which shows the pores at every other layer except the surface elements. Fig. 3 shows the pores' distribution in the simulated three-dimensional solid.

The analysis options used for simulation were: large displacement, constant dilatation and large strain additive.

4 DISCUSSION

During the plastic deforming process of tensile samples, there are two factors that affect the results. One factor is the hardening characteristic of metal, the more the sample is elongated, the harder it becomes. In other words, the appropriate yield function depends not only on the level of the deviatoric stresses but also the hydrostatic stresses[2, 3]. The deforming hardening of material improves the deforming resistance, which leads to the larger load. The other factor is the geometry softening characteristic of material. The reduction of cross-section area leads to the lower load bearing. On the even plastic deforming stage, the factor of hardening plays an important role. With the increase of deformation, the cross-section shrinks gradually, so the influence of geometry softening increases evidently.

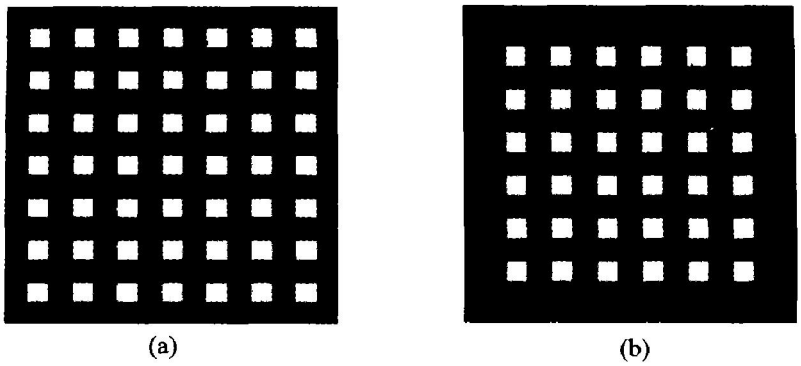

Fig. 2 Pores' distribution assumption
(a) —Distribution of pores at odd layers; (b) —Distribution of pores at even layers

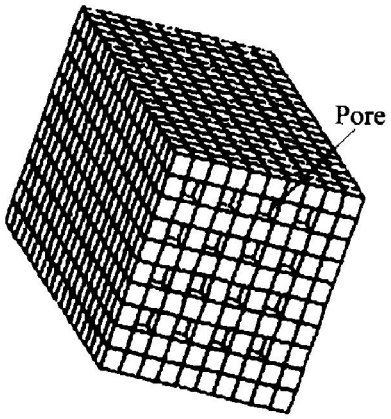

Fig. 3 Distribution of pores in three-dimensional solid

Fig. 4 shows the curves of load versus displacement obtained from both simulation and experiment. Firstly, the material properties of three-dimensional solid for tensile simulation were defined with reference to the known pure iron parameters[2]. The material behavior was assumed to be elasto-plastic with elastic modulus E = 210 GPa and Poisson's ratio γ = 0.27. The initial yield stress is 200 MPa. The workhardening curve is described in Fig. 5.

From the comparison of pure iron simulation and experimental results, we can say that the existence of voids induced the stress concentration although the sample was sintered. The stress concentration may cause the fracture under low nominal pressure.

Secondly, the elastic modulus was adjusted to 15 000 MPa while the Possion's ratio was still unchanged. As shown in Fig. 4, the slope in the elastic stage agrees well with the experimental result.

Finally, the elastic modulus was adjusted to 15 000 MPa and the Possion's ratio was adjusted to 130 MPa. The simulation results show good accordance with the experimental results.

Fig. 6 shows the contour line of equivalent von Mises stress distribution. No apparent necking is found during the tension process. In iron-base sintered materials, with the aggravation of local plastic deformation and spread of crack, the yield strength of materials is gradually reduced. The stress concentration and strength decline are mainly caused by factors such as increase of voids irregularity and decrease of voids curvature.

5 CONCLUSIONS

1) In iron - base sintered materials, the exist-

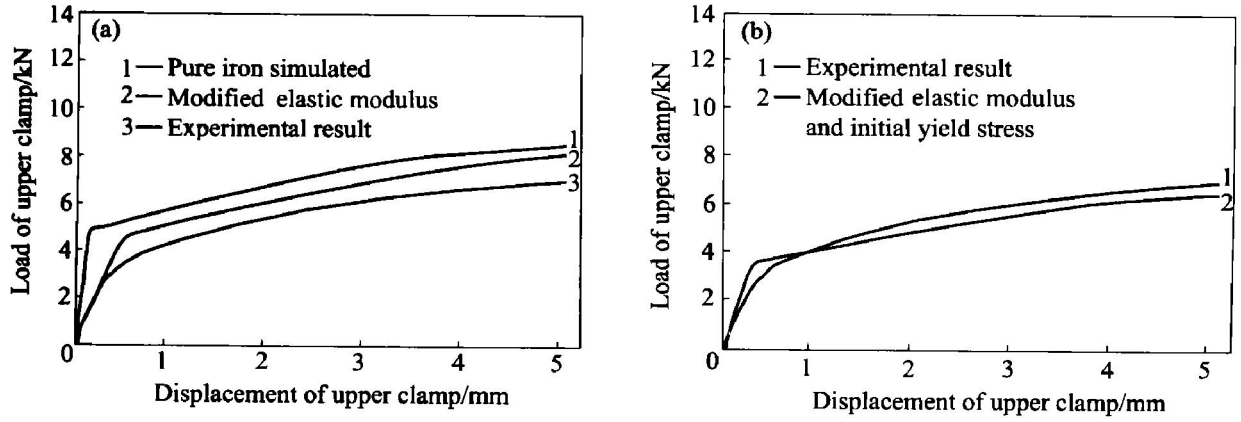

Fig. 2 Plot of load versus displacement
(a) —Pure iron simulated; (b) —Modified elastic modulus and initial yield stress

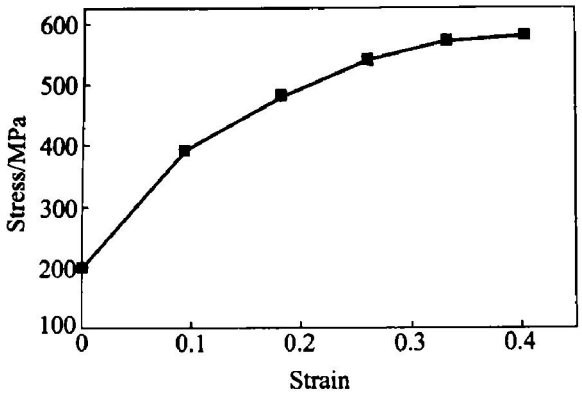

Fig. 5 Workhardening curve

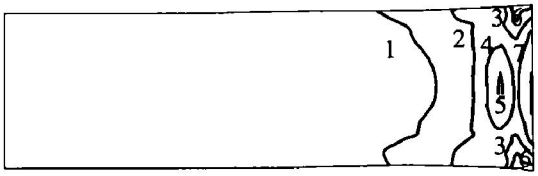

Fig. 6 Contour line of equivalent von Mises stress

1 —316.1 MPa; 2 —299.5 MPa; 3 —284.6 MPa; 4 —271.5 MPa; 5 —246.3 MPa; 6 —315.4 MPa; 7 —274.1 MPa

ence of voids and crack leads to local plastic deformation, thus reduces elastic modulus and the yield strength. The simulation adopting pure iron material properties shows considerable error. When adjusting the material properties including elastic modulus and initial yield stress, the obtained results show good agreement with the experimental results.

2) The model presents an effective assumption of designing voids in three-dimensional iron-base sintered materials. With this assumption, both the random distribution of voids and the initial relative density needed by the tensile simulation are ensured.

[REFERENCES]

[1] LI Yuan-yuan, ZHANG Da-tong, XIAO Zhi-yu, et al. Influence of high-energy ball milling on Al-30% Si powder and ceramic particulate [J]. Trans Nonferrous Met Soc China, 2000, 10(3): 324-327.

[2] LI Yuan-yuan, Ngai Tungwai Leo, XIAO Zhi-yu, et al. A study on mechanical property of warm compacted iron-based materials[J]. J Cent South Univ Technol, 2002, 9(3): 154-158.

[3] LI Yuan-yuan, XIAO Zhi-yu, Ngai Tungwai Leo, et al. On warm compacted NbC particulate reinforced iron-base composite Ⅰ: effect of fabrication parameters[J]. Trans Nonferrous Met Soc China, 2002, 12(4): 659-663.

[4] LI Yuan-yuan, XIAO Zhi-yu, Ngai Tungwai Leo, et al. On warm compacted NbC particulate reinforced iron-base composite Ⅱ: effect of fabrication parameters[J]. Trans Nonferrous Met Soc China, 2002, 12(4): 664-668.

[5] Li Y Y, Ngai T L, Zhang D T, et al. Effect of die wall lubrication on warm compaction powder metallurgy[J]. Journal of Material Processing Technology. 2002, 129(1-3): 354-358.

[6] Zhou Z Y, Chen Z Y, Zhao W B. Densification model for porous metallic powder materials[J]. Journal of Material Processing Technology, 2002. 129(1-3): 385-388.

[7] Zhou Z Y, Zhao W B, Chen P Q. Simulation of die wall friction's effect on density distribution in metallic powder compaction[J]. Trans Nonferrous Met Soc China, 2002, 12(5): 890-893.

[8] Tran D V. Numerical modeling of powder compaction processes: displacement based finite methods[J]. Powder Metallurgy, 1993, 36(4): 257-263.

[9] Shima S, Oyane M. Plasticity theory for porous metals[J]. Int J Mech Sci, 1976, 18, 285-292.

[10] Doraivelu S M. A new yield function for compressible P/M materials[J]. Int J of Mech Sci, 1984, 26(9/10): 527-535.

[11] Tamura S. Three dimensional granular modeling for metallic powder compaction and flow analysis[J]. J of Material Processing Technology, 1994, 42: 197-207.

[12] Lian J. Powder assembly simulation by particle dynamics methods[J]. Inter J For Numerical Methods in Engineering, 1994, 37: 763-775.

[13] CHENG Y F, GUO S J, LAI H Y. Dynamic simulation of random packing of spherical particles[J]. Powder Technology, 2000, 107: 123-130.

[14] Mori K, Shima S. Finite element method for the analysis of plastic deformation of porous metals[J]. Bull JSME, 1980, 23(178): 12-18.

[15] Schofield A N. Original cam-clay[A]. International Conference on Soft Soil Engineering[C]. Guangzhou, 1993. 8-11.

[16] MSC Company. MSC Marc 2000 User's Guide[M]. Software Corporation, 2000.

(Edited by PENG Chao-qun)